Chinese Chemical Letters 33 (2022) 2442–2446

Contents lists available at ScienceDirect

Chinese Chemical Letters

journal homepage: www.elsevier.com/locate/cclet

Circularly polarized luminescence based on cholesterol-tetraphenylethylene-perylene liquid crystal

Shengjie Jiang[a,b], Shujuan Zhou[a], Ying Chen[a], Hongyu Guo[a,b], Fafu Yang[a,c,*]

[a] College of Chemistry and Materials Science, Fujian Normal University, Fuzhou 350007, China
[b] Fujian Key Laboratory of Polymer Materials, Fuzhou 350007, China
[c] Fujian provincial Key Laboratory of Advanced Materials Oriented Chemical Engineering, Fuzhou 350007, China

ARTICLE INFO

Article history:
Received 8 May 2021
Revised 14 October 2021
Accepted 18 October 2021
Available online 23 October 2021

Keywords:
Tetraphenylethylene
Perylene
Circularly polarized luminescence
Liquid crystal
FRET

ABSTRACT

Perylene derivative with circularly polarized luminescence (CPL) at aggregated state was seldom reported due to the strong ACQ (aggregation-caused quench) effect at aggregation. In this work, a novel cholesterol-tetraphenylethylene-perylene derivative (**TPE-P**) was designed and synthesized in moderate yield. It exhibited liquid crystalline behavior with orderly hexagonal columnar mesophase and good fluorescence emission at long wavelength (600-700 nm) not only in solution but also at aggregated states based on the AIE (aggregation-induced emission)-FRET (fluorescence resonance energy transfer) effect between tetraphenylethylene unit and perylene moiety. Moreover, the circular dichroism (CD) and CPL studies suggested the effective chiral transfer from cholesterol unit to tetraphenylethylene unit and perylene skeleton due to the spiral liquid crystalline self-assembly. The CD and CPL signals showed the order of THF < THF-hexane < solid film < meosphase, indicating that the higher spiral orderly degree resulted in the stronger chiral transfer. The largest $|g_{lum}|$ value for mesophase excited at 320 nm was as high as 1.5×10^{-2} based on the combining effect of AIE-FRET and chiral transfer. This research not only reported a novel CPL perylene derivative at aggregated state, but also confirmed that the combination of AIE-FRET effect and chiral transfer of liquid crytalline phase was an effective method to construct normal dye with excellent CPL property in aggregated state.

In recent years, circularly polarized luminescence (CPL) materials had exhibited great application prospect in novel chiral display materials such as chiral light-emitting transistors, optical information storage and processing, color image projection, and 3D displays [1–11]. CPL reflects the chiral information of the fluorescent material at excited state, which not only depends on the chiral characteristic of single molecule, but also is usually decided by the molecular self-assemble behavior at aggregated state. Through self-assembly of chiral molecules, the helical aggregates could be obtained, which can further transfer and/or amplify the CPL properties of chiral materials. On the other hand, liquid crystal was the well-known molecular aggregate with the orderly self-assemble system. At present, studies have shown that chiral light-emitting liquid crystals can be formed by doping chiral molecules in commercial liquid crystal molecules to afford a stable chiral configuration [12]. The chiral liquid crystalline materials with CPL properties were also reported in some cases [13–24]. Although the remarkable progress had been achieved in liquid crystals with CPL properties, however, the design and synthesis of novel CPL liquid crystalline materials based normal fluorescence dyes with good CPL emission at aggregated state was still a challenging work.

Perylene diimide (PDI) derivatives, as typical excellent chromophores with strong long-wavelength emission, have been used as effective building blocks for design and synthesis of CPL emission materials [25–33]. For examples, Cheng's group reported circularly polarized luminescence of chiral perylene diimide with D/L alanine moiety [34]. Zeng *et al.* prepared diagonally π-extended perylene-based bis(heteroacene) with CPL activity [36]. Miguel and co-worker synthesized a simple perylene diimide cyclohexane derivative bearing CPL and two-photon absorption (TPA) properties [37]. Wang group presented CPL materials based on PDI-embedded double [8] helicenes [38]. Although these chiral perylene derivatives exhibited good CPL properties in solution, they usually showed weak even no CPL emission in aggregate states due to the strong aggregation-caused quench (ACQ) effect. On the other hand, it was well-known that the aggregation-induced emission (AIE) was the opposite luminescence phenomenon of ACQ effect, exhibiting good fluorescence emission at aggregate states.

* Corresponding author.
E-mail address: yangfafu@fjnu.edu.cn (F. Yang).

https://doi.org/10.1016/j.cclet.2021.10.050
1001-8417/

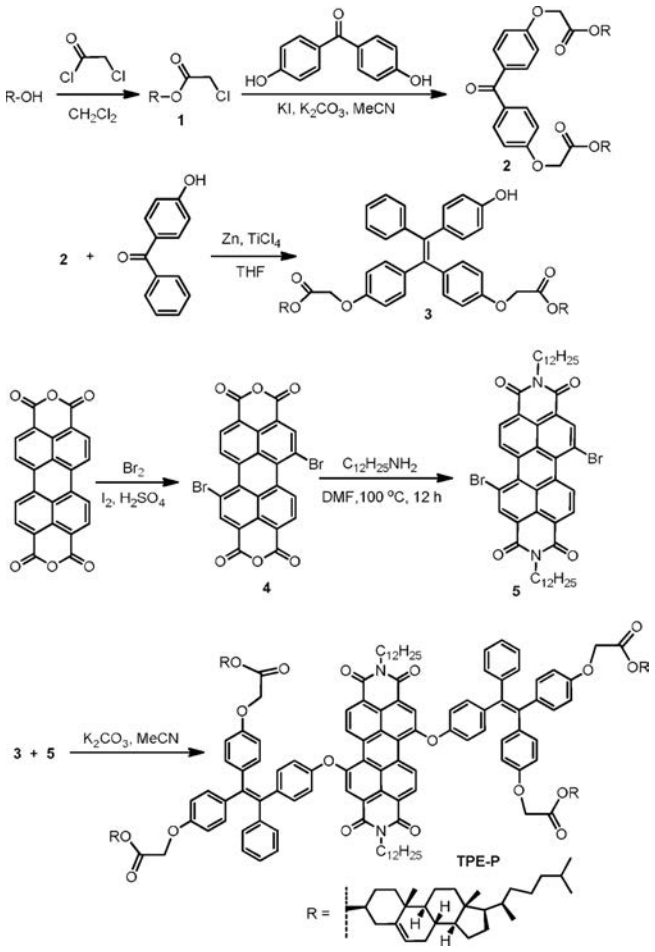

Scheme 1. The synthetic route for title compound **TPE-P**.

The AIE molecules with good CPL properties had been also constructed successfully by grafting chiral groups on AIE moieties [38–40]. Recently, our group prepared several perylene liquid crystals with excellent solid fluorescence by introducing AIE groups onto perylene skeleton [41,42], supplying a new strategy for designing perylene derivative with CPL property at aggregate states. Inspired by this successful attempt, in this paper, a novel PDI liquid crystal with cholesterol (chiral unit)-tetraphenylethylene (AIE unit)-perylene (emitting skeleton) structure was designed and synthesized. This PDI material displayed good CPL emission at aggregated states based on the effective chiral transfer of spiral orderly liquid crystalline self-assembly and the AIE-FRET (fluorescence resonance energy transfer) effect between tetraphenylethylene and perylene unit, which was firstly observed for PDI derivative.

As perylene liquid crystals had been confirmed extensively as orderly self-assembly aggregates [43–55], four cholesterol units and two dodecyl units were introduced on the periphery of perylene to form the orderly liquid crystalline self-assembly. On the other hand, tetraphenylethylene was the typical AIE emitting unit at aggregated state. Its emission wavelength (400-600 nm) overlapped with the absorption wavelength (440-600 nm) of PDI skeleton, suggesting the possibility of AIE-FRET effect between these two moieties. The synthetic route was designed as Scheme 1. Firstly, hydroxyl-tetraphenylethylene derivative **3** with two cholesterol units was prepared by reacting compound **2** with hydroxybenzophenone under typical reaction condition of Zn-$TiCl_4$/THF system. Secondly, according to the published procedure [41], by bromination reaction with Br_2 and then ammonolysis with dodecylamine, perylene tetracarboxylic anhydride was smoothly transferred to compound **5** in yield of 65%. Finally, by treating compounds **3** and **5** in K_2CO_3/MeCN system, the target compound (**TEP-P**) was obtained in 76% yield after column chromatography. The structure of **TPE-P** was confirmed by FT-IR, ^{1}H NMR, ^{13}H NMR, MALDI-TOF-MS and elemental analysis. All analysis data were well in consistent with the structure (Supporting informaiton). For example, a singlet and two doublets were distinguished for PDI skeleton, suggesting the symmetrical substituent of two tetraphenylethylene units on perylene skeleton.

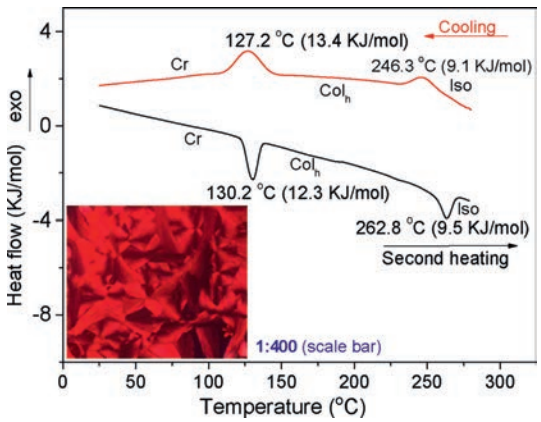

Fig. 1. DSC curves of **TPE-P** upon second heating and first cooling. Inserted picture: The liquid crystalline texture under POM at 150 °C (×400 times).

Firstly, the liquid crystalline property of **TPE-P** was investigated with the assistance of differential scanning calorimetry (DSC), polarizing optical microscope (POM) and X-ray diffraction (XRD). Fig. 1 showed the DSC curve of **TPE-P** upon the second heating and the first cooling. The corresponding thermal data were summarized in Table S1 (Supporting information). It can be seen in Fig. 1 that two endothermic peaks were observed at 130.2 °C and 262.8 °C during the second heating, and two exothermic peaks appeared at 127.2 °C and 246.3 °C on cooling. These reversible thermal transition peaks corresponded to the phase transition characteristics of crystalline-mesophase-isotropic phase. Due to the large molecular weight with a certain viscosity, these DSC curves exhibited broad peaks and a slight hysteresis on cooling. Furthermore, POM was used to observe the mesomorphic texture of **TPE-P**. During the heating and cooling process, significant phase changes of Iso-Col and Col-Cr were distinguished. The liquid crystalline texture under POM observation at 150 °C was exhibited as the inserted picture of Fig. 1. The typical focal-fan texture indicated the hexagonal columnar mesophase, which was further confirmed by the following XRD analysis.

Next, the molecular packing behavior of **TPE-P** at mesophase was studied by XRD analysis. As shown in Fig. 2, a sharp scattering peak and two weak emission peaks appeared at 2θ = 2.34°, 4.05° and 4.68°, respectively. These small angles indicated the d-spacings of 37.72, 21.80 and 18.87 Å, which corresponded to the ratio of 1:$\sqrt{3}$:2. Therefore, these d-spacings could be indexed as [d_{100}], [d_{110}] and [d_{200}] of columnar hexagonal mesophase. Also, a wide diffusion halo of the molten alkyl chain at 2θ = 15-32° was observed in the wide-angle region, indicating the average distance of 4.2 Å. A weak reflection at 24.67° (distance of 3.61 Å) indicated the intracolumnar core-core distance for the hexagonal columnar mesophase. All these XRD data supported the hexagonal columnar liquid crystal for **TPE-P**. On the other hand, the calculated value of the lattice parameter (a) was 43.55 Å based on the XRD data, which was smaller than the linear diameter of **TPE-P** (approximately 66 Å). This result might imply that the peripheral alkyl units were folded, curled or interdigitation at mesophase.

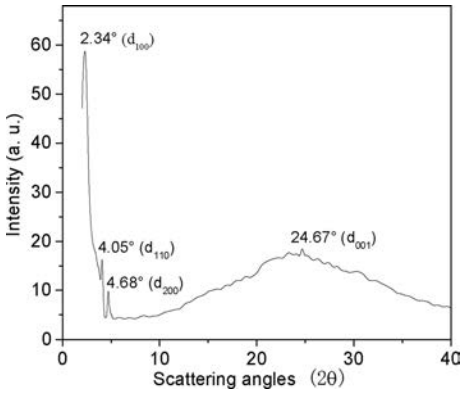

Fig. 2. The XRD trace of **TPE-P** at 150 °C for mesophase.

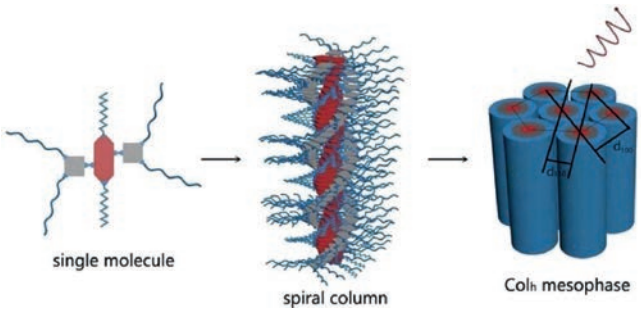

Fig. 3. The proposed spiral molecular stacking of Col_h mesophase of **TPE-P**.

Moreover, according to the formula of $n_{cell} = (a^2)(\sqrt{3}/2)(h\rho N_A/M)$ to calculate the average molecular number in per column (where *a*, N_A and *M* were recognized as the lattice parameter, Avogadro's number and molecular mass, respectively), n_{cell} was estimated as 1.11 (near 1). Therefore, the possible molecular stacking mode of the hexagonal column for **TPE-P** was shown in Fig. 3, in which one slice was composed of one molecule, and the self-assembly of these chiral molecules produced the spiral columnar morphology (Further CD and CPL investigation supported this spiral columnar behavior).

The photophysical properties of **TPE-P** were studied by UV-vis spectra and fluorescence spectra, and compared with that of precursors **3** and **5**. The UV-vis spectra of compounds **3** (AIE unit), **5** (perylene without AIE moiety) and **TPE-P** were exhibited in Fig. S9 (Supporting information). It can be seen that **TPE-P** possessed the absorption peaks at 512 and 550 nm, which were the typical absorption band of perylene skeleton. In addition, **TPE-P** showed a strong absorption peak at 309-360 nm, which was consistent with the absorption of compound **3**. These phenomena indicated that the perylene and TPE units in **TPE-P** exhibited their respective UV-vis absorption characteristics. Fig. S10 (Supporting information) displayed the fluorescence spectra of compound **5** and **TPE-P** in THF solution. Both of them had two fluorescence emission peaks at 550-700 nm. The obvious red shift of fluorescence emission for **TPE-P** in comparison with compound **5** was ascribed to the increasing push-pull effect and larger aromatic-conjugated structure after the substitution of Br by TPE units. **TPE-P** exhibited the higher fluorescence intensity than compound **5**, which could be attributed to the bigger steric hindrance of TPE units reducing the ACQ effect of the perylene units.

The AIE performance of **TPE-P** and reference compounds **3** and **5** were further investigated in the THF-hexane mixtures. As shown in Fig. S11 (Supporting information), with the increase of hexane fraction, compound **3** displayed the gradual increasing fluorescence at 400-600 nm, indicating the excellent AIE effect for compound

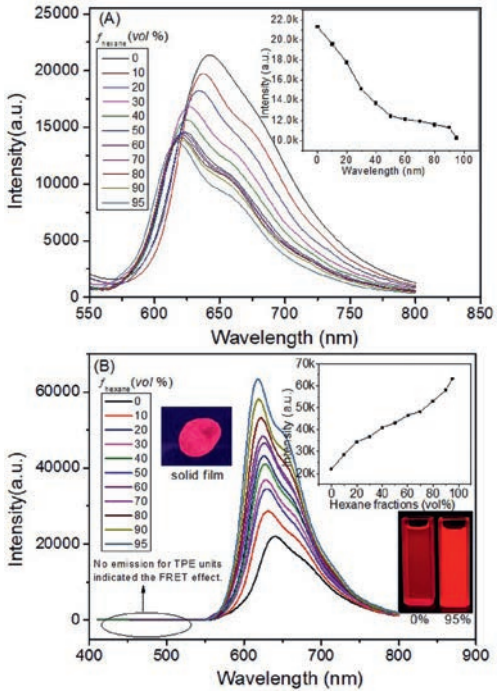

Fig. 4. (A) The fluorescence spectra of **TPE-P** (1 mol/L) in the THF-hexane with different hexane fractions (λ_{ex} = 510 nm). (B) The fluorescence spectra of **TPE-P** (1 mol/L) in the THF-hexane with different hexane fractions (λ_{ex} = 320 nm). Inserted: The picture of solid film and the plot of fluorescence intensities *vs.* hexane fractions and the fluorescence photos (under UV_{365} light) of **TPE-P** in THF-hexane mixtures with f_{hexane} = 0% and 95%, respectively.

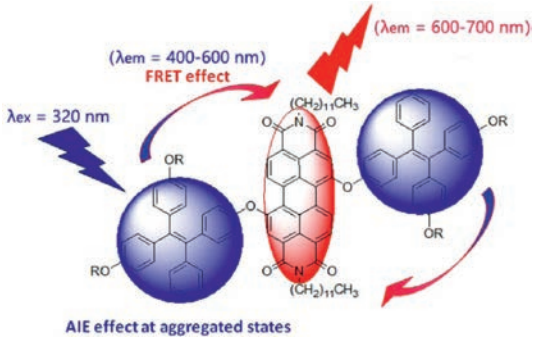

Fig. 5. The proposed illustration of the AIE-FRET effect for **TPE-P**.

3. However, with the increase of hexane fraction, the fluorescence of compound **5** decreased obviously (Fig. S12 in Supporting information), suggesting the ACQ effect which was in accordance with normal perylene derivatives. Since the fluorescence emission (400-600 nm) of compound **3** in aggregate state overlapped with the absorption band of the perylene skeleton of **TPE-P** (450-600 nm), the AIE-FRET effect was expected between TPE and perylene unit. As illustrated in Fig. 4A, when excited at 510 nm (the absorption of perylene skeleton), the fluorescence of **TPE-P** decreased with the increase of hexane fractions. On the other hand, Fig. 4B showed the opposite fluorescence change with excitation wavelength at 320 nm (the absorption of TPE unit), in which the fluorescence intensities of **TPE-P** increased remarkably with the increase of hexane fractions. The highest fluorescence intensity at f_{hexane} = 95% increased by three times in comparison with that in pure THF solution. The obvious blue shift of maximum emission wavelength might be ascribed to the decrease of polarity and TICT effect with the increase of hexane fractions in THF-hexane mixtures. Moreover, no obvious fluorescence emission between 400 nm and 500

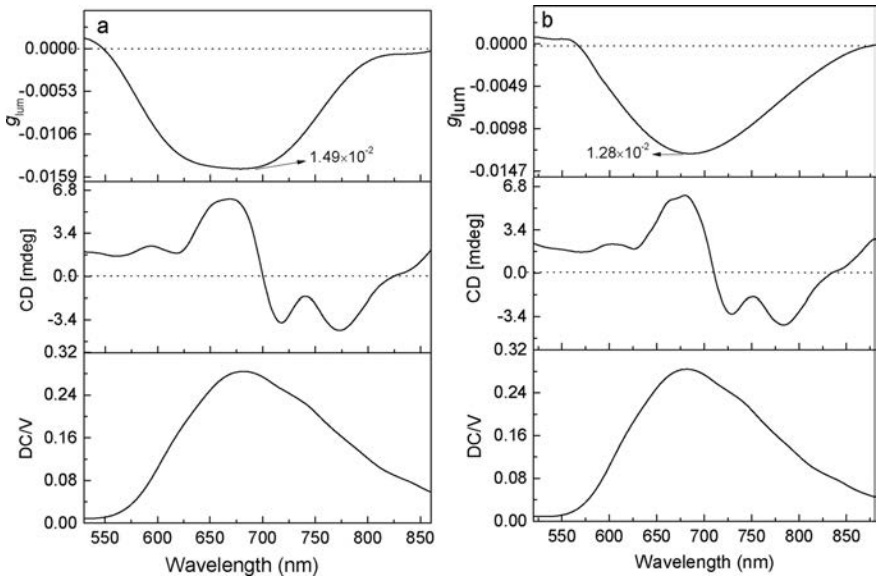

Fig. 6. CPL spectra of **TPE-P** at mesophase (150 °C). (a) λ_{ex} = 320 nm. (b) λ_{ex} = 510 nm.

nm was observed for the TPE units in aggregated state. These phenomena certainly supported the AIE-FRET effect for **TPE-P** in THF-hexane solution. When excited at 320 nm for the absorption of TPE unit, TPE unit exhibited AIE effect with fluorescence emission at 400-600 nm (as shown in Fig. S11), which was further transferred to perylene skeleton, resulting in the disappearance of emission at 400-600 nm and the increasing emission for perylene skeleton (600-700 nm). According to the definition of energy transfer efficiency ($\Phi_{ET} = 1 - I_{DA}/I_D$, where I_{DA} is the fluorescence intensity when the donor is present, and I_D is the fluorescence intensity of the donor when there is no acceptor), the calculated energy transfer efficiency was 90.8%. The AIE-FRET effect was further supported by the fluorescence spectra at the aggregated states of solid film and mesophase (simulation method by treating the film of **TPE-P** on quartz plate for 30 min at 150 °C for its columnar phase and then examining the emission rapidly at room temperature). As shown in Fig. S13 (Supporting information), compound **5** possessed no emission in solid film but **TPE-P** had good fluorescence emission at both solid film and mesophase although a little decrease of fluorescence was observed at mesophase. These results were in accordance with the above AIE-FRET effect. Also, one can see that fluorescence wavelength at solid film and mesophase showed obvious red shift in comparison with that in solution, which might indicate the *J*-aggregation at solid film and mesophase. The absolute fluorescence quantum yields (excited at 320 nm) of **TPE-P** in THF solution, solid film and mesophase were 0.11, 0.32 and 0.28, respectively. By comparing with the previous weak emission for perylene derivatives in solid states [34–37], **TPE-P** exhibited the excellent fluorescence in aggregated states. According to the above analysis, the possible AIE-FRET emission mechanism of **TPE-P** was proposed as Fig. 5.

Since **TPE-P** was surrounded by four chiral cholesterol moieties, it was expected to exhibit the circular dichroism (CD) and CPL property based on the orderly helical self-assembly at aggregated states. Firstly, CD spectra were employed to investigate the chiral information of **TPE-P** in the ground state. As displayed in Fig. S14 (Supporting information), with the increase of hexane fractions in THF-hexane mixtures, the CD signals changed obviously. When f_{hexane} < 80%, **TPE-P** showed the silent CD signal in the absorption zone. But when f_{hexane} > 80%, **TPE-P** aggregates exhibited the obvious CD signals at about 300-350 nm and the strong CD signals between 450 nm to 580 nm (including the positive Cotton effect at 530 nm and the negative Cotton effect at 483 nm). These CD signals were consistent with the absorption zone of TPE units and perylene skeleton (by comparing with the UV-vis absorption spectra of **TPE-P**, Fig. S15 in Supporting information), indicating the chiral characteristic was successfully transferred from cholesterol units to TPE and perylene skeleton. Furthermore, the CD spectra of **TPE-P** in solid film and mesophase were studied. As shown in Fig. S16 (Supporting information), **TPE-P** showed the positive Cotton effect at 450-600 nm. By comparing with all these CD signal, it could be concluded that they showed the order of THF < THF-hexane < solid film < meosphase. These results were in accordance with the orderly aggregated degree. In THF solution, the good solubility resulted in little aggregation. In THF-hexane mixtures, the aggregation degree was enhanced gradually with the increase of hexane fractions. In solid film, the orderly degree of aggregation increased obviously based on the slow evaporation of solvent on quartz glass. At mesophase, **TPE-P** exhibited the strongest CD signal due to the formation of orderly spiral hexagonal columnar mesophase. All these results confirmed that the chiral could be transferred and amplified based on the spiral self-assemble system of liquid crystal as expected.

Table 1
The CPL data of **TPE-P**.

Phase states	λ_{em}	Φ_f[d]	g_{lum}[e]	g_{lum}[f]
THF	642	0.11	weak	weak
THF-hexane[a]	615	0.26	-4.8×10^{-3}	-4.3×10^{-3}
Solid film[b]	680	0.32	-7.2×10^{-3}	-5.1×10^{-3}
Mesophase[c]	694	0.28	-1.5×10^{-2}	-1.3×10^{-2}

[a] THF-hexane mixture with 95% of hexane.
[b] The THF solution of **TPE-P** was dropped onto the quartz glass and then the solvent was volatilized to obtain the solid film.
[c] Mesophase at 150 °C.
[d] Fluorescence absolute quantum yield excited at 320 nm.
[e] λ_{ex} = 320 nm.
[f] λ_{ex} = 510 nm.

Furthermore, the CPL property of **TPE-P**, reflecting the chirality at excited state, was studied in four typical aggregated states (pure THF solution, THF-hexane with 95% of hexane, solid film and mesophase). The results were presented in Fig. 6 and Figs. S17-S19 (Supporting information). The corresponding CPL data were summarized in Table 1. As can be seen that no obvious CPL signal was

detected in the THF solution, but the remarkable CPL emissions were observed in the aggregated states of THF-hexane mixtures, solid film and mesophase. The CPL signals also showed the order of THF < THF-hexane < solid film < meosphase, which were in consistent with that of CD signals. As **TPE-P** possessed the AIE-FRET effect, the CPL emission at excited at both 320 nm and 510 nm were explored. The results suggested that the asymmetry factor (g_{lum}) of CPL properties excited at 320 nm were bigger than that excited at 510 nm. These phenomena could be explained by that the good AIE-FRET effect enhanced the CPL emission of perylene skeleton. The largest $|g_{lum}|$ value for mesophase excited at 320 nm was as high as 1.5×10^{-2}, which was outstanding among all kinds of CPL perylene derivatives [24–35]. Based on these CD and CPL analyses, the spiral columnar morphology for aggregated state, especially for liquid crystalline state could be proposed in Fig. 3 (middle part of spiral column). It was worthy of noting that **TPE-P** was the first perylene CPL material at aggregated state based on the effective chiral transfer of spiral orderly liquid crystalline self-assembly and the AIE-FRET effect.

In conclusion, a novel perylene derivative (**TPE-P**) with cholesterol (chiral unit)-tetraphenylethylene (AIE unit)-perylene (emitting skeleton) structure was designed and synthesized in moderate yield. Its liquid crystalline behaviour was studied and the orderly hexagonal columnar mesophase was proposed. Moreover, the AIE-FRET effect between tetraphenylethylene unit and perylene skeleton was confirmed. **TPE-P** exhibited good fluorescence emission in both solution and aggregated states. The obvious CD and CPL signals were observed in aggregated state with the order of THF < THF-hexane < solid film < meosphase, indicating that the higher spiral orderly degree resulted in the stronger chiral transfer. The largest $|g_{lum}|$ value was 1.5×10^{-2} for mesophase excited at 320 nm. This research not only reported a novel perylene derivative with good CPL property, but also supplied an effect method to construct normal dye derivative with good CPL property at aggregated states based on the combination of AIE-FRET effect and chiral transfer of orderly spiral self-assembly of liquid crystal.

Declaration of competing interest

The authors declare that they have no known competing financial interests or personal relationships that could have appeared to influence the work reported in this paper.

Acknowledgments

Financial support from the National Natural Science Foundation of China (No. 21406036), Fujian Science and Technology Project (No. 2019N0010), and the National Undergraduate Innovation Program in Fujian Normal University (No. cxxl-2021300) were greatly acknowledged.

Supplementary materials

Supplementary material associated with this article can be found, in the online version, at doi:10.1016/j.cclet.2021.10.050.

References

[1] Y.J. Zhang, T. Oka, R. Suzuki, J.T. Ye, Science 131 (2014) 725–728.
[2] R. Carr, N.H. Evans, D. Parker, Chem. Soc. Rev. 41 (2012) 7673–7686.
[3] Z.C. Shen, T.Y. Wang, L. Shi, Z.Y. Tang, M.H. Liu, Chem. Sci. 6 (2015) 4267–4272.
[4] M. Gong, R. Sawada, Y. Morisaki, Y. Chujo, Macromolecules 50 (2017) 1790–1802.
[5] H.Z. Zheng, W.R. Li, W. Li, X. Wang, et al., Adv. Mater. 30 (2018) 1705948.
[6] F. Song, Z. Zhao, B.Z. Tang, et al., J. Mater. Chem. C 8 (2020) 3284–3301.
[7] M. Li, L.J. Chen, Y. Cai, et al., Chem 5 (2019) 634–648.
[8] S. Huo, P. Duan, T. Jiao, Q. Peng, M. Liu, Angew. Chem. Int. Ed. 129 (2017) 12342–12346.
[9] C. Wang, T. Jiang, X. Ma, Chin. Chem. Lett. 31 (2020) 2921–2924.
[10] D. Zhang, C.Y. Yu, L. Zheng, et al., Chin. Chem. Lett. 31 (2020) 673–676.
[11] Y.L. Yan, X.L. Li, K.Z. Tang, et al., Chin. Chem. Lett. 32 (2021) 107–112.
[12] K. Liu, Y.H. Shen, X.J. Li, et al., Chem. Comm. 56 (2020) 12829–12832.
[13] S. Jiang, J. Qiu, Y. Chen, H. Guo, F. Yang, Dyes. Pigm. 159 (2018) 533–541.
[14] H. Li, J. Cheng, H. Deng, et al., J. Mater. Chem. C 3 (2015) 2399–2404.
[15] Q. Ye, D. Zhu, H. Zhang, X. Lu, Q. Lu, J. Mater. Chem. C 3 (2015) 6997–7003.
[16] S. Chen, S. Jiang, J. Qiu, H. Guo, F. Yang, Chem. Commun. 56 (2020) 7745–7748.
[17] F. Song, Z. Xu, Q. Zhang, et al., Adv. Funct. Mater. 28 (2018) 1800051.
[18] S. Jiang, J. Qiu, L. Lin, H. Guo, F. Yang, Dyes. Pigm. 163 (2019) 363–370.
[19] F. Song, Y. Cheng, Q. Liu, et al., Mater. Chem. Front. 3 (2019) 1768–1778.
[20] J. Liu, H. Su, L. Meng, Y, et al., Chem. Sci. 3 (2012) 2737–2747.
[21] J.C.Y. Ng, J. Liu, H. Su, et al., J. Mater. Chem. C 2 (2014) 78–83.
[22] H. Li, J. Cheng, Y. Zhao, et al., Mater. Horiz. 1 (2014) 518–521.
[23] Q. Liu, Q. Xia, S. Wang, B.S. Li, B.Z. Tang, J. Mater. Chem. C 6 (2018) 4807–4816.
[24] H. Li, B.S. Li, B.Z. Tang, Chem. Asian J. 14 (2019) 674–688.
[25] T. Ikeda, T. Masuda, T. Hirao, et al., Chem. Commun. 48 (2012) 6025–6027.
[26] F. Würthner, C.R. Saha-Möller, B. Fimmel, et al., Chem. Rev. 116 (2016) 962–1052.
[27] J. Kumar, T. Nakashima, H. Tsumatori, T. Kawai, J. Phys. Chem. Lett. 5 (2014) 316–321.
[28] T. Kawai, K. Kawamura, H. Tsumatori, et al., ChemPhysChem 8 (2007) 1465–1468.
[29] J. Kumar, T. Nakashima, H. Tsumatori, et al., Chem. Eur. J. 19 (2013) 14090–14097.
[30] H. Tsumatori, T. Nakashima, T. Kawai, Org. Lett. 12 (2010) 2362–2365.
[31] J. Kumar, T. Nakashima, T. Kawai, Langmuir 30 (2014) 6030–6037.
[32] J. Kumar, H. Tsumatori, J. Yuasa, T. Kawai, T. Nakashima, Angew. Chem. Int. Ed. 54 (2015) 5943–5947.
[33] J. Li, C. Yang, X. Peng, et al., Org. Biomol. Chem. 15 (2017) 8463–8471.
[34] F. Li, Y. Li, G. Wei, et al., Chem. Eur. J. 22 (2016) 12910–12915.
[35] B. Li, W. Peng, S. Luo, et al., Org. Lett. 21 (2019) 1417–1421.
[36] P. Reine, A.M. Ortuño, I.F.A. Mariz, D. Miguel, et al., Front. Chem. 8 (2020) 306–312.
[37] B. Liu, M. Böckmann, W. Jiang, N.L. Doltsinis, Z. Wang, J. Am. Chem. Soc. 142 (2020) 7092–7099.
[38] J. Li, J. Wang, H. Li, et al., Chem. Soc. Rev. 49 (2020) 1144–1172.
[39] Z. Zhao, H. Zhang, J.W.Y. Lam, B.Z. Tang, Angew. Chem. Int. Ed. 59 (2020) 9888–9907.
[40] H.T. Feng, J.W.Y. Lam, B.Z. Tang, Coord. Chem. Rev. 406 (2020) 213142.
[41] Zhu M, Zhuo Y, Cai K, Guo H, F. Yang, Dyes Pigm. 147 (2017) 343–349.
[42] M. Zhu, Y. Chen, X. Zhang, et al., Soft. Matter. 14 (2018) 6737–6744.
[43] L. Lu, H.J. Sun, Y.T. Zeng, Y. Shao, et al., J. Mater. Chem. C 8 (2020) 10422–10430.
[44] V. Grande, B Soberats, Herbst S, V. Stepanenko, F. Würthner, Chem. Sci. 9 (2018) 6904–6911.
[45] S.C. Tan, J.Y. Tao, W.L. Luo, et al., Chin. Chem. Lett. 32 (2021) 1149–1152.
[46] L. Meng, Q. Wu, F. Yang, H. Guo, New J. Chem. 39 (2015) 72–76.
[47] Q. Wei, L. Shi, H. Cao, et al., Chin. Chem. Lett. 18 (2007) 527–529.
[48] C. Keum, D. Becker, E. Archer, et al., Adv. Optical Mater. 8 (2020) 2000414.
[49] M. Zhu, Z. Wang, F. Yang, H. Guo, Dyes Pigm. 133 (2016) 387–394.
[50] R.K. Gupta, A.A. Sudhakar, Langmuir 35 (2019) 2455–2479.
[51] M. Zhu, H. Guo, F. Yang, Z. Wang, Rsc. Adv. 7 (2017) 4320–4328.
[52] Y.Z. Zhao, D. Wang, Z.M. He, et al., Chin. Chem. Lett. 26 (2015) 185–789.
[53] F. Würthner, C.R. Saha-Möller, B. Fimmel, et al., Chem. Rev. 116 (2016) 962–1052.
[54] J. Lin, X. Ji, H. Guo, F. Yang, J. Mol. Liq. 290 (2019) 111228.
[55] X. Zhang, H. Guo, F. Yang, J. Yuan, Tetrahedron Lett. 57 (2016) 905–909.